Research Article

Lucie Costes, Mario Aguedo, Loic Brison, Sylvain Brohez, Aurore Richel, Fouad Laoutid*

Lignin fractionation as an efficient route for enhancing Polylactide thermal stability and flame retardancy

Abstract: Due to its variable botanical origin, functionality, reactivity, and heterogeneity, using lignin in industrial application is not an easy task. In the present study, we investigate the effect of lignin fractionation as a simple way for reducing the variability in its properties. Kraft lignin was separated by ultrafiltration membranes in two fractions with a specific molecular weight and the properties of each fraction were characterized through FTIR, XPS, TGA and cone calorimeter test. Lignin fractions display different thermal and combustion behaviors. Thus, the two fractions have been evaluated as flame retardant additives for polylactide (PLA). PLA composites, containing well dispersed lignin (20 wt%), were produced by melt blending in an internal mixer. The thermo-degradant effect of each fraction on PLA during melt processing was investigated by rheological analysis and size exclusion chromatography while the composites thermal stability and fire properties were evaluated using TGA and cone calorimeter test. Results showed that using appropriate lignin fraction enables for obtaining PLA composites presenting enhanced properties

*Corresponding author: Fouad Laoutid, Laboratory of Polymeric & Composite Materials, Materia Nova Research Center - University of Mons UMONS, Place du Parc 23, B-7000 Mons, Belgium, E-mail: fouad.laoutid@materianova.be
Lucie Costes, Loic Brison, Laboratory of Polymeric & Composite Materials, Materia Nova Research Center - University of Mons UMONS, Place du Parc 23, B-7000 Mons, Belgium
Mario Aguedo, Aurore Richel, Laboratory of Biological and Industrial Chemistry, University of Liège - Gembloux Agro-Bio Tech, Passage des Déportés, 2 B-5030 Gemblou, Belgium
Sylvain Brohez, Service de Génie des Procédés Chimiques; Faculté Polytechnique - University of Mons UMONS, Place du Parc 23, B-7000 Mons, Belgium

1 Introduction

Lignin, which is the second most abundant constituent of the biomass making up to 10–25% of lignocellulosic biomass, presents some interesting properties that allows its use as a sustainable flame retardant additive for polymeric materials. In fact, thanks to its aromatic structure, lignin presents the ability to form some char under pyrolysis and fire conditions that can induce some reduction of the burning rate.

The use of lignin as flame retardant additive in polymeric materials has been reported in many papers [1-10] and some of them reported that lignin flame retardant effect is mainly affected by its nature [1, 6].

Lignin structure and properties are variable and are influenced by many parameters [11]. Lignin contains a wide variety of functional groups (methoxy, phenolic hydroxyl, aldehyde, and carboxylic acid groups) and different bond types [12]. Its complex structure is composed of a cross-linked 3D network of three different phenylpropanoid units, i.e. p-hydroxyphenyl (H), guaiacyl (G) and syringyl (S). The composition in the different units of lignin is strongly dependent on the botanical sources. Guaiacyl lignin is generally found in softwoods, while guaiacyl-syringyl lignin is more present in hardwoods. [13].

The extraction of lignin from the other ligno-cellulosic constituents is possible through different industrial processes, divided into two categories: with sulfur and sulfur-free processes [14]. Sulfur treatments result in the production of black liquor which is acidified to recover lignin, such as kraft and lignosulfonate lignins. Sulfur-free lignins, such as organosolv lignin and soda lignin, are recovered by precipitation after solvent pulping or after alkaline pulping. These processes affect differentially lignin structure and its chemical composition [15]. Kraft

lignin generally contains chains of lower molecular weight and less sulfur than lignosulfonate lignin. Kraft lignin also holds a high amount of condensed structures and a large number of phenolic hydroxyl groups because of the β-aryl bond cleavage occurring during the cooking process. Sulfur-free lignins, such as organosolv lignin and soda lignin have lower molecular weight and Tg than kraft lignin.

Lignin botanical origin and its extraction process affect its thermal stability [16-18] that begins to decompose between 150°C and 275°C and continues up to 700°C with the formation of stable charred residues, representing 30 to 50% of the initial dry weight under inert atmosphere [19-22]. However, lignin thermal degradation is a complex mechanism that can be influenced also by other parameters, such as the thermal conditions [23] and the presence of other components [24].

Thus, due to its high structural diversity and large molecular weight distribution, using lignin in industrial application is a hard task. The size of the lignin molecules can vary from some hundred to few thousand g/mol within the same sample. Lignin fractionation into specific fractions presents one of the best ways to produce lignin presenting reduced variability in terms of size, reactivity and composition.

Lignin fractionation can be performed mainly through three methods, i.e. differential precipitation by decreasing gradually the pH of the solution, using selective solvents for the lignin extraction or by using membrane technology [**25**]. Among these three methods, ultrafiltration allows obtaining lignin fractions with defined molecular weight distributions without using any reagents.

In this work, we investigated for the first time, the effect of lignin fractionation on the thermal stability and the flame-retardant behavior of PLA based composites. Two lignin fractions derived from the same kraft lignin, presenting different average molecular weights, have been obtained by ultrafiltration. The attributes of these fractions and their effect upon PLA properties were investigated by several characterization techniques. Lignin fractionation appears to present an interesting pathway for limiting its thermo-degradant effect on PLA and enhancing its flame retardant behavior.

2 Experimental

2.1 Materials

PLA resin (3051D) with a number average molecular weight of 100 000 g/mol, a dispersity of 2.1 and 4.3 % of D-lactide content was purchased from NatureWorks. Two lignin fractions, obtained by ultrafiltration of a kraft lignin were used in this study. After membrane separation, both lignins were washed in order to decrease the content in total salts. They were then dried and ground into a fine powder.

2.2 Melt processing

Blending of lignin within the molten PLA was carried out in a Brabender internal mixer at 160°C (7 min mixing at 70 rpm). PLA and lignins were previously dried in a vacuum oven at 60°C overnight right before use. Plates (100*100*4 mm³) for cone calorimeter testing were compression-molded at 160°C using an Agila PE20 hydraulic press and following a precise pressure program: the sample is first deposited for 3 min on the hot part, it is then pressed for 3 min 20 s at 10 bars, followed by 3 degassings, it is then pressed again for 2 min 30 s at 150 bars, and finally the sample is deposited in the cold part where it is pressed for 5 min. PLA alone and PLA composites containing 20 wt% of each lignin fraction were prepared.

2.3 Characterizations

2.3.1 Thermal analysis

Thermal decomposition of the different lignins, pristine PLA and PLA-based composites were studied by thermogravimetric analysis (TGA). Approximately 10 mg of the sample was submitted to a temperature ramp from 100 to 700°C at a heating rate of 20°C/min after a 10 min isothermal at 100°C to get rid of any moisture. All TGA experiments were performed under a nitrogen flow of 90 ml/min using a TGA Q50 device from TA Instruments.

2.3.2 Structural characterizations

Fourier transform infrared (FTIR) spectra were recorded using a Bruker IFS 66V/S spectrometer. Spectra were recorded using a spectral width ranging from 600 to 4000 cm⁻¹, with 4 cm⁻¹ resolution and an accumulation of 32 scans.

X-ray photoelectron spectroscopy (XPS) analyses were carried out with a Phi 5000 Versa Probe apparatus (Spot RX de 200 μm). The monochromatic source was Al Kα X-ray (1486.6 eV). The percentage of each element present has been determined at low-resolution scan (Epass =

187.85 Ev) while a high-resolution scan (Epass = 23.35 Ev) has been used for determining the types of bonds and their concentrations.

Size exclusion chromatography (SEC) was used to determine the number average molecular weights of both PLA and PLA/lignin blends. The number average molecular weights and molecular weight distributions were determined in $CHCl_3$ at 23°C using an Agilent size exclusion chromatograph equipped with a Knauer 2320 refractometer index detector and two PLGel columns (MIXED-D and 10^3A). Samples were dissolved in $CHCl_3$ (5 mg/1 ml), 20 μL of the solutions were injected into the columns using a flow rate of 1 mL/ min. Monodisperse polystyrene standards (Polymer Laboratories Ltd.) were used for the primary calibration.

Besides, the peak average molecular weights of lignins were evaluated by using a high-performance size exclusion chromatography (HPSEC) with UV detection at 280 nm. The HPLC system (Waters 2690) (Waters Inc., Milford, MA, USA) was equipped with a pre-column and two TSKgel GMPWxl columns in series (300 mm x 7.8 mm) with particles sizes of respectively 7 and 6 μm (Tosoh Co. Ltd., Tokyo, Japan), and coupled on-line with UV detection (Waters 996 Photodiode array detector). The eluent solution contained 6.9 g $NaH_2PO_4.H_2O$ and 3.2 g NaOH in distilled water and the pH was adjusted to 12 with 6 M NaOH. Before use, it was filtrated on 0.45 μm and sonicated during 15 min. The calibration was made with a range of poly(4-styrenesulfonic acid) ammonium salts (PSS-Na) with mass average molecular weights from 208 a/mol to 77.4 kg/mol. PSS-Na and lignins were dissolved in a volume of eluent, at 1 mg/mL and 3 mg/mL respectively. Before analyses, the lignin solutions were kept under magnetic stirring during 48 h to ensure a complete dissolution and then filtered on a 0.45 μm nylon filter. Elution was carried out at 30°C, at a flow rate of 0.9 mL/min.

Morphological investigation was performed to highlight the dispersion state of lignin in PLA using a scanning electron microscopy (SEM) Hitachi SU8020 (100 V–30 kV) apparatus. PLA composites were cryo-fractured after immersion in liquid nitrogen and then coated using a gold sputtering technique to avoid any charging effect during the electron beam scanning.

Non-cellulosic total monosaccharides composition was determined through gas chromatography after total hydrolysis of the samples with 1 M H_2SO_4 and acetylation. No-cellulosic polysaccharides were converted into monosaccharides by hydrolysis in H_2SO_4 (1 M) at 100°C during 3 h. The free monosaccharides were then derivatized by 1-methylimidazole and acetic anhydrid into alditol acetates prior to gas chromatography analysis, as previously described [25]. Analyses were carried out using an Agilent (7890 B series) gas chromatograph. The components were separated using a capillary column, HP1-methylsiloxane (30 m × 0.32 mm ID, 0.25 m film thickness). Helium was used as carrier gas at a flow rate of 1.6 mL min–1. Injection chamber was set at 290°C, and the temperature program was 1 min at 120°C, followed by a linear increase in 4 min to 220°C and then in 35 min to 290°C which was maintained for 4 min. Compounds were detected using a flame ionization detector at 320°C. Data were analyzed using OpenLab ChemStation software. Glucose, xylose, arabinose, mannose, rhamnose, galactose and 2-deoxyglucose (internal standard) were purchased at Sigma-Aldrich (St.-Louis, USA). The anhydro correction factors (0.88 for pentoses and 0.90 for hexoses) were applied to the monomeric sugars concentrations in order to obtain the concentration of the corresponding polymeric sugars.

2.3.3 Fire behavior characterization

The effect of both fractions on PLA fire behavior was investigated by using cone calorimeter at 35 kW/m². Cone calorimeter is one of the most used device to assess the flammability of materials at bench scale. The peak of heat release rate (pHRR) as well as time to ignition (TTI), that are considered as two of the most important parameters in this fire test, have been considered. A high pHRR and a low TTI may cause both fast ignition and rapid-fire propagation. Cone calorimeter tests were performed according to ISO 5660 standard procedures with a FTT cone calorimeter. Samples (100*100*4 mm³) were exposed to an external heat flux of 35 kW/m², corresponding to common heat flux in a mild fire scenario. Cone calorimeter tests were also performed on compacted lignin powder (10 g) under 35 kW/m².

3 Results and discussion

3.1 Structural, thermal and fire properties of lignin fractions

3.1.1 Average molecular weight of the lignin fractions

The two lignin fractions were characterized by high performance size exclusion chromatography (HPSEC) coupled to UV detection. Results, presented in Fig 1 evidence that the ultrafiltration process enables for a clear

separation of lignin in two fractions with different average molecular weights, i.e. a low molecular weight fraction (LMW fraction) composed of populations with the highest peak at 2660 g/mol, and a high molecular weight fraction (HMW fraction), exhibiting an average molecular weight of around 5109 g/mol.

3.1.2 Structural characterization

FTIR spectroscopy was performed to compare the chemical composition of both fractions. FTIR analysis reveals that both lignin fractions, originated from the same Kraft black liquor, contain similar functional groups (Fig. 2). The two spectra are very similar. The absorbance of the peak located at (3400 cm^{-1}), and corresponding to phenolic and aliphatic O-H stretching vibration, is very weak, indicating that the two fractions contain few O-H groups. Moreover, GC-MS analysis reveal the presence of some hemicellulose that has not been evidenced by FTIR analysis because if its low content, i.e. 2.52% ± 0.04 in

HML fraction and 0.39% ± 0.05 in LMW fraction. It is worth mentioning that the amount of hemicellulose is higher in the HMW fraction because of its branched structure.

In order to further investigate the surface of both fractions, we used XPS to determine the atomic percentage of each element as well as the type of bonds and their concentrations. Results are shown in **Fig. 3** and **tables 1** and **2**. The survey spectra (**Fig 3** and **table 1**) reveal that C and O are the predominant species at the surface of both fractions and gave an O/C atomic ratio of 0.33 and 0.26 for low and high molecular weight fractions respectively. This result indicates that LMW fraction contains more oxidant groups at it surface. This result is confirmed by high-resolution scans of C1s spectra, curve-fitted with C-C, C-O and C=O peaks, that clearly evidence the presence of more oxidized C in LMW fraction (**Table 2**). It is worth mentioning that XPS analysis reveals the presence of low amount of sulfur, due to the use of sodium sulfide during the Kraft extraction process. Some -OH lignin groups are replaced by sulfonyl groups. However, sulfur content has been found to be more than two times higher in LMW fraction.
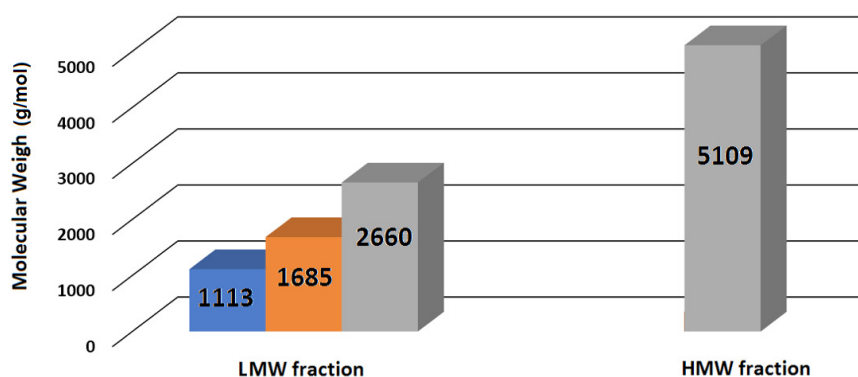

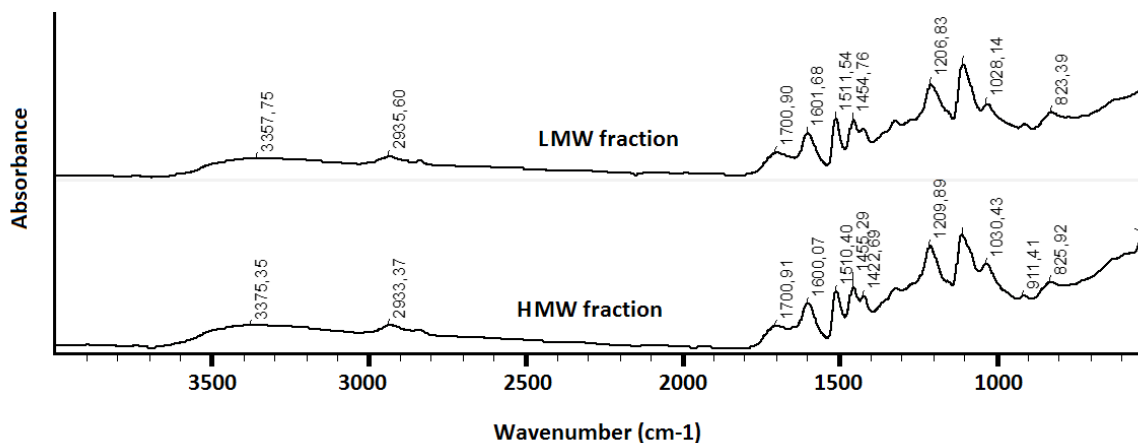**Figure 1:** Average molecular weight (in g/mol) of the two lignin fractions.

Figure 2: FTIR spectra of the two lignin fractions.
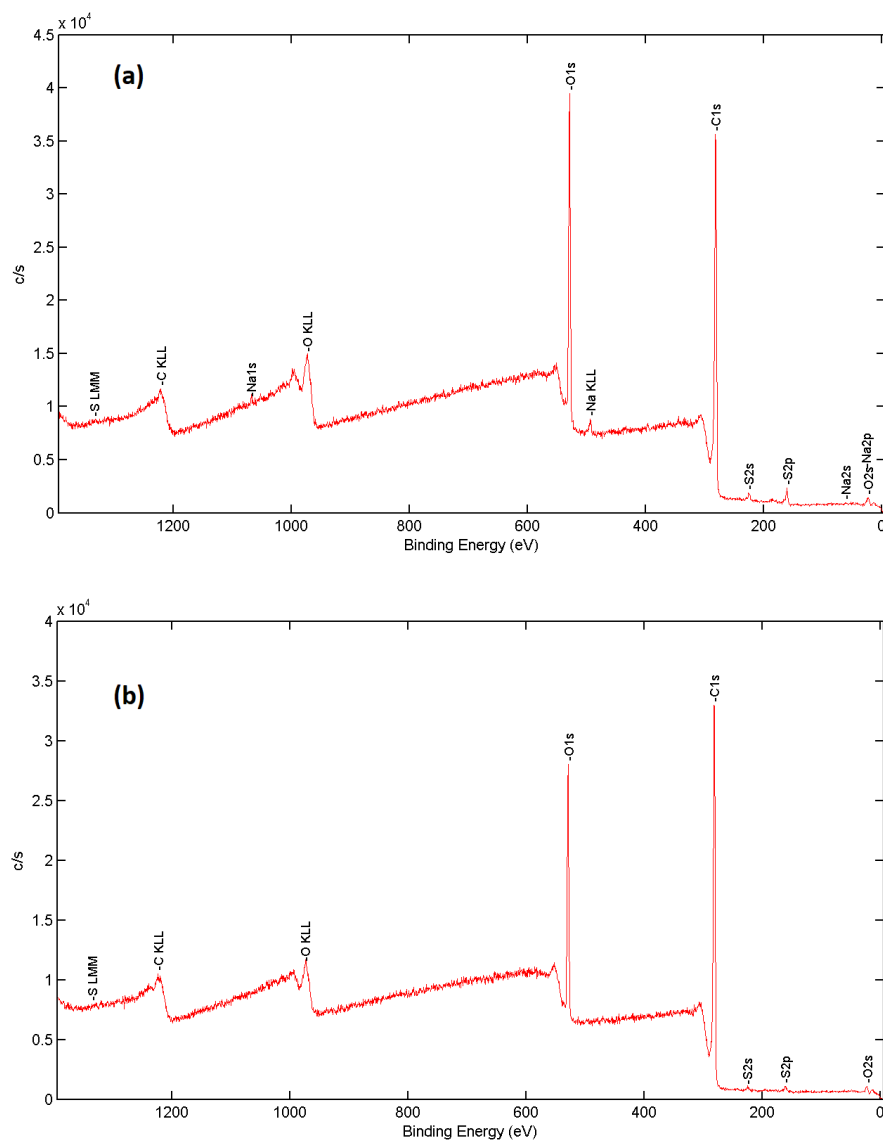
Figure 3: XPS survey spectra of LMW fraction (a) and HMW fraction (b).

Table 1: XPS binding energy (BE), C1s, O1s S2p atomic percentages of elements as well as the O/C ration for both fractions.

	C1s	O1s	Na	S2p	O/C
Low MW fraction	73.64	24.49	0.46	1.41	0.33
High MW fraction	78.64	20.74	---	0.61	0.26

Table 2: XPS binding energy (BE), C-C, C-O and C=O Atomic percentages chemical bonds for both fractions.

	C-C (BE=284.8 eV)	C-O (BE=286.3 eV)	C=O (BE=289 eV)
Low MW fraction	51.7	45.8	2.5
High MW fraction	59.35	39.4	1.3

3.1.3 Thermal degradation

TGA curves of both fractions are presented in **figure 4** and summarized in **table 3**. Both fractions start to decompose above 200°C ($T_{-5\%}$ = 220°C and 270°C for LMW and HMW fractions respectively). This information is very important since it means that both fractions could be processed with PLA at 160°C.

Lignin thermal degradation is relatively well described in the literature [**18**]. After moisture release, the first decomposition step occurs between 230 and 260°C corresponding to propanoid side chains cleavage that leads to the formation of low molecular weight products. This first step is followed by the main degradation (275–350°C) that leads to the production of a large quantity of methane due to the cleavage of the main chain by either C–C and β-β scission or by aryl-ether cleavage. Above 500°C, the formation of char takes place thanks to further rearrangements and condensation of the aromatic structure, which thermal decomposition starts at 650°C.

According to TGA results, HMW fraction display higher thermal stability. The higher is lignin molecular weight, the higher is its thermal stability. Temperatures corresponding to the weight loss of 10%, 20% and 40% are respectively 256, 316, 366°C for LMW fraction and 313, 360, 422°C for HMW fraction (**Table 3**). The effect of molecular weight on lignin thermal stability has also been reported by Mousavioun and Doherty [**26**]. In their study, authors evidenced that low molecular weight soda lignin fraction started to degrade at lower temperatures than higher molecular weight fractions. Authors concluded that the reduction of the thermal stability of low molecular weight fraction is due to its chemical structure, composed by few polyphenolic compounds and containing a high carboxylic acid amount. This conclusion supports our XPS results that indicated that LMW fraction contains higher amount of oxidant groups that HMW fraction.

Wang et al [**27**] reported similar conclusions. They evidenced that the thermal stability of different Kraft lignin fractions increased with the average molecular weight. The enhanced thermal stability of high molecular weight fractions has been attributed to their long and branched structures that are more difficult to volatilize in comparison with the small fragments. The formation of small molecular weight is due to the oxidative reactions taking place during kraft process while high molecular weight fractions result from the condensation and
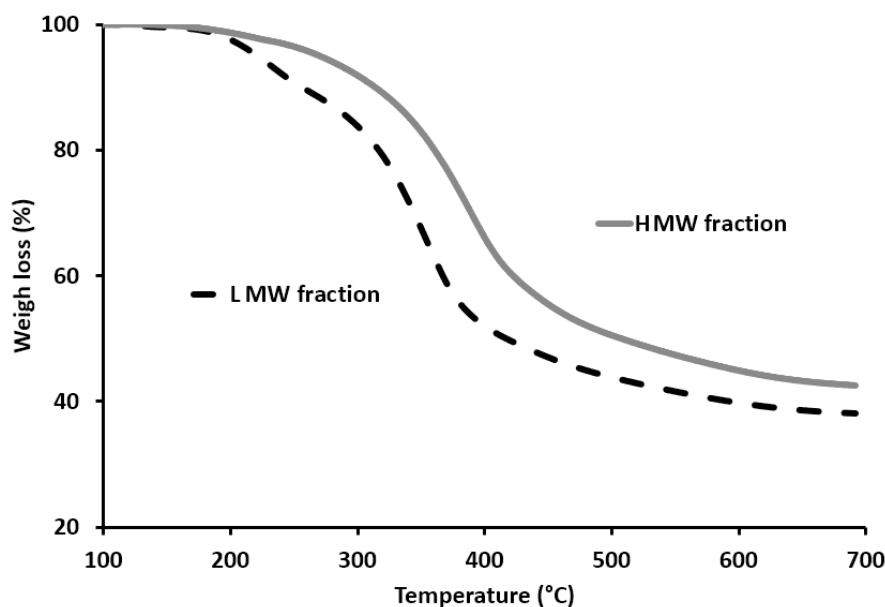
Figure 4: effect of lignin molecular weight on TG curves under nitrogen at 20°C/min.

Table 3: Thermogravimetric data of the two lignin fractions.

	$T_{-5\%}$	$T_{-10\%}$	$T_{-20\%}$	$T_{-40\%}$	Residue at 600°C (%)
Low MW fraction	220	256	316	366	40
Hight MW fraction	270	313	360	422	45

recombination reactions involving the formation of stable carbon-carbon bonds

These results indicate that besides the well-known parameters, which are botanical origin, extraction process, number of reactive functions, presence of catalyst ..., lignin molecular weight is an important parameter that can affect its thermal behavior.

The amount of the final residue formed at 600°C is not strongly affected by lignin molecular weight since the amounts of the remaining products are very close (40 % for low MW fraction and 45 % for high MW fraction.

3.2 Thermal stability and fire performances of the composites

3.2.1 Dispersion state

20 wt% each lignin fractions were incorporated into PLA by melt blending. Since the dispersion state of the additives significantly impacts the final properties of composite materials, we investigated first the quality of dispersion of both fractions in the composite by SEM. It can be observed on **Fig. 5** that the dispersion state of both fractions is similar without the presence of large aggregates. However, some decohesion is evidenced around lignin particles indicating poor interfacial adhesion between PLA and lignin particles.

3.2.2 Thermal stability

The effect of lignin fractionation on PLA thermal stability was investigated. Lignin thermo-degradant action on PLA has been reported to start at relatively low temperatures (during melt processing at 160°C) and induces significant reduction of the polymer chain molecular weight [11]. This thermo-degradant effect can also be maintained at higher temperatures and results in a decrease of the composite thermal stability during TGA analyses.

In order to access the effect of the incorporation of lignin fractions on PLA thermal degradation during melt processing, the number average molecular weights of PLA chains in processed PLA and PLA – lignin compositions were determined by using Size exclusion chromatography (SEC).

Results, presented in **table 4**, evidence a reduction of PLA chain average molecular weight in the presence
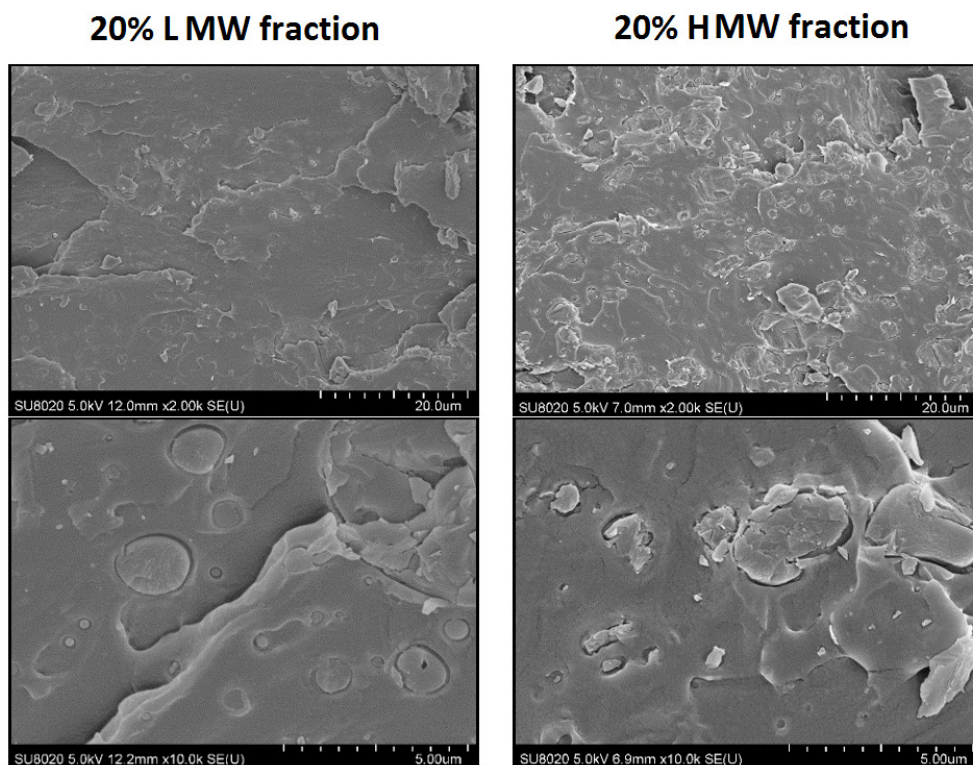

Figure 5: SEM pictures of PLA containing 20 wt% low and high molecular weight fractions.

of both fractions but this degradant effect is more limited when high MW fraction is used. This result clearly demonstrates the important degradant effect of the oxidant groups, present at the surface of lignin particles (evidenced by XPS analysis). In fact, LMW lignin fraction contains higher amount of oxidant groups at its surface than HMW one.

The degradation induced during melt processing was also evidenced by rheological analysis. **Fig. 6** shows the plot of dynamic viscosity (Eta*) against the angular frequency for pristine PLA and PLA/lignin composites. It can be observed that the incorporation of both lignin fractions induces some reduction of the blend viscosity, resulting from the decrease of polymer chain molecular weight. Viscosity of the composite containing LMW fraction is lower than that containing HMW fraction. The viscosity evolution follows thus the same trend than PLA molecular weights measurement.

At higher temperature, the thermo-degradant effect of lignin during TGA analysis depends on the nature of the fraction used. **Fig. 7** presents pyrolytic decomposition of PLA containing 20 wt% low- and high-MW lignin fractions. Interestingly, only LMW fraction induces a premature thermal degradation of PLA. HMW fraction does not affect the composite thermal stability. The

PLA premature thermal degradation observed could be directly related to the thermal stability of lignin. In fact, low thermally stable lignin (LMW fraction) starts to degrade at lower temperature (220°C for $T_{-5\%}$) (**Table 3**) and thus induces PLA thermal degradation. In contrast, the high MW fraction, that is more thermally stable (270°C for $T_{-5\%}$) induces limited PLA thermal degradation. Indeed, the temperature corresponding to 5 % weight loss ($T_{-5\%}$) of the later composite (326°C) is very close to that of pristine PLA (334°C), while this temperature is recorded at lower temperature (286°C) when low MW fraction is used (**Table 5**).

In order to be able to determine whether the reduction of the composites thermal resistance in the presence of LMW fraction is due to the lower thermal stability of this fraction, it is necessary to calculate additive TGA responses (theoretical curves) and compare them with the experimental curves. Two theoretical curves have been calculated by considering TG curves of PLA as well as both lignin fractions under nitrogen. Fig. 7 showed theoretical TG curves of PLA – lignin composites in comparison with the experimental curve of pristine PLA.

From these results, it can be clearly established that the degradant interaction between LMW fraction and PLA is responsible for the reduction of the composite

Table 4: Results of SEC analysis on processed PLA and related composites recorded after melt processing

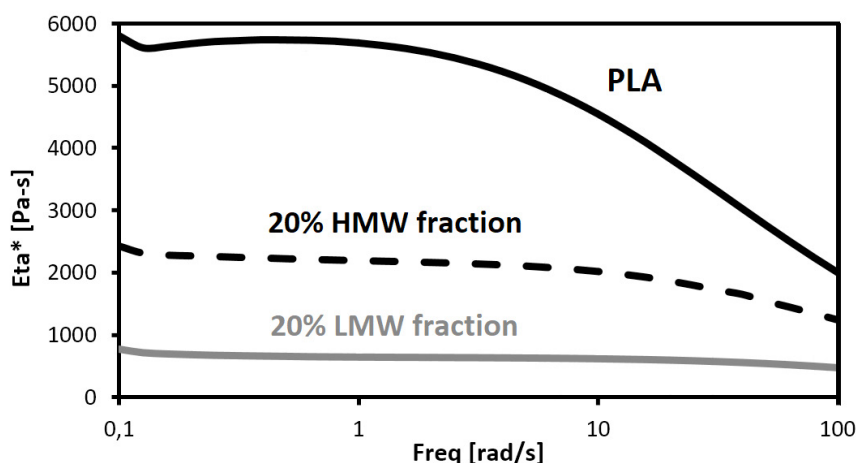|	Mn (g/mol)	Mw (g/mol)	Mw/Mn
Processed PLA	85000	169200	2,0
PLA/20 Low MW fraction	55000	112900	2,1
PLA/20 High MW fraction	65700	133900	2,0

Figure 6: Effect of the lignin molecular weight on the dynamic viscosity of PLA composites in comparison with pristine PLA.

thermal stability during TGA analysis. In fact, contrary to experimental TGA curves, theoretical ones are similar whatever the nature of lignin fraction used. Moreover, apart from a slight premature thermal degradation of the composites, corresponding to less than 20% weight loss and occurring below 350ºC, theoretical curves do not reveal any significant shift to lower temperatures when lignin fractions are used.

In conclusion, these results demonstrate that lignin fractionation presents an interesting way for reducing the thermo-degradant effect of lignin at both low and high temperatures. On the first hand, thanks to the separation of the small fragments containing more reactive oxidized sites on their surfaces, the HMW fraction leads to limited polymer degradation during melt processing as it was demonstrated by both SEC (**Table 4**) and rheological analysis (**Figure 6**). On the second hand, removing these less thermally stable fragments enables for limiting PLA premature thermal degradation during TGA experiments (**Figure 7**).

Moreover, the presence of 20 wt% lignin, whatever its molecular weight, results in the formation of some char residue (around 6%) at 800ºC. For sake of comparison, pristine PLA degrades entirely without formation of any residue.

3.2.3 Fire behavior

HRR and mass loss curves are presented in **Fig. 8** and the pictures of the residues in **Fig. 9**. Results summarized in **table 6**. Pristine PLA exhibits a strong combustion, starting after 87 s, consuming all the material and releasing a total heat of 92 MJ/m² with a pHRR of 390 kW/m². In addition to the composite thermal stability, the incorporation of both fractions triggers different modifications of the composites fire behavior. As it can be observed on **Fig. 8** and **table 6**, both fractions increase the composite ignitability. In fact, time to ignition decreases from 87 s for pristine PLA to 68 s in the presence of lignin, whatever the nature of the fraction used. Similar effect of lignin has been reported in PBS [1] and ABS [3] and PLA [6, 11, 28] and was attributed to the combined effect of both the
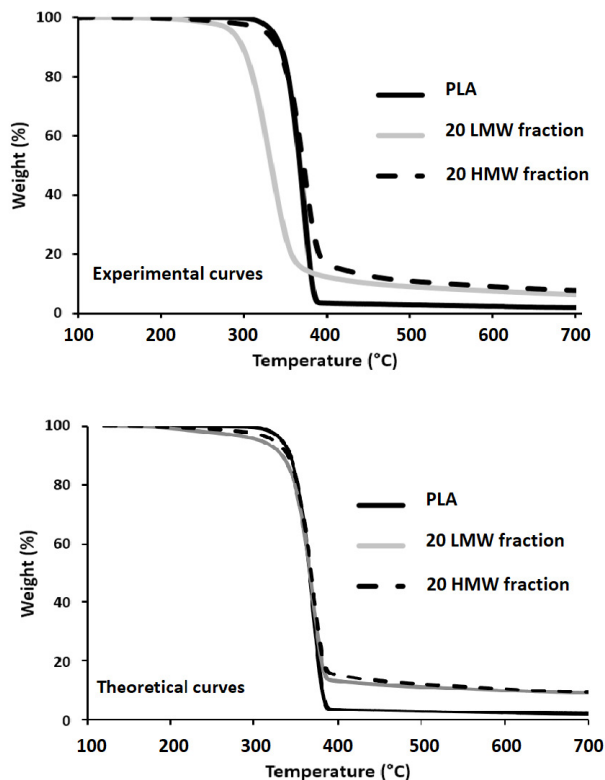

Figure 7: Experimental and theoretical TG curves of PLA/20 wt% lignin compositions compared to the thermal behavior of neat PLA (under N2, 20ºC/min).

modification of the heat absorption and earlier release of combustible products. An increase of the heat absorption of the material, due to its black coloration, was suggested to promote the ignition by inducing a stronger heating of the decomposition gases. Moreover, both fractions demonstrate a high ignitability during cone calorimeter test performed on 10 g of compacted lignin powders (**Fig. 11**). In fact, time to ignition of both fractions is very low (30 s) and the incorporation of such easily flammable product could lead to a faster composite ignition.

However, only HMW fraction enables for significant reduction of pHRR from 390 kW/m² for pristine PLA to 266 kW/m². In comparison, using 20 wt% LMW fraction does not lead to any change of pHRR that remains very close to

Table 5: Thermogravimetric data of PLA/Lignin blends.

	T$_{-5\%}$	T$_{-10\%}$	T$_{-20\%}$	T$_{-40\%}$	Residue at 800ºC
PLA	334	340	353	366	2
PLA / Low MW fraction	286	298	310	325	5.6
PLA / Hight MW fraction	326	340	353	366	7

that of pristine PLA (362 kW/m²). Moreover, a significant change of the HRR curve shape is noticed when HMW fraction is used. HRR curve of this composition contains a second HRR peak (around 350 s) corresponding to the char cracking. In comparison with pristine PLA, a premature mass loss during cone calorimeter test is observed in the presence of both fractions (**Fig. 8**). This behavior is due to the fast ignition of the composites that promotes its thermal decomposition. However, the mass loss rate is strongly reduced when HMW fraction is used thanks to the formation of the char layer.

The incorporation of lignin, whatever the nature of the fraction used, does not affect THR that remains close to that of pristine PLA (**Table 6**). In the case of PLA containing HMW fraction, the high THR value obtained is due to the extension of the combustion peak and to the presence of the second HRR peak. Indeed, the second peak corresponds to the char collapse allowing further release of combustible products.

To further investigate the effect of each fraction on the composites flame retardant behavior, we investigate the fire properties of each fraction during cone calorimeter test. 10 g of each fraction were compacted and deposited into the cone calorimeter pan and submitted to the cone calorimeter test following the same parameters as for the composites (35 kW/m²). HRR curves obtained (**Fig. 10**) show that LMW fraction exhibits a strong combustion with a PHRR reaching 540 kW/m² while low peak of about 230 kW/m² is obtained during the combustion of HMW fraction. Small lignin fragments, that are more easily

volatilized as attested by TGA experiments (Fig 4), are responsible for the intense combustion of LMW fraction. It is therefore obvious that the incorporation of such high combustible fraction into PLA matrix could not contribute positively for reduction peak reduction. In addition, the thermo-degradant effect of LMW fraction that induces some PLA premature thermal degradation is likely to contribute of the increase of the PHRR.
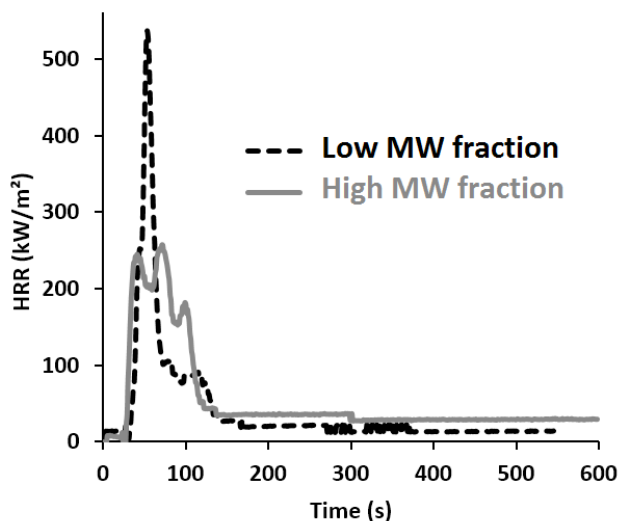

Figure 10: Cone calorimeter curves of low and high molecular weight lignin fractions.

20 % Low MW fraction
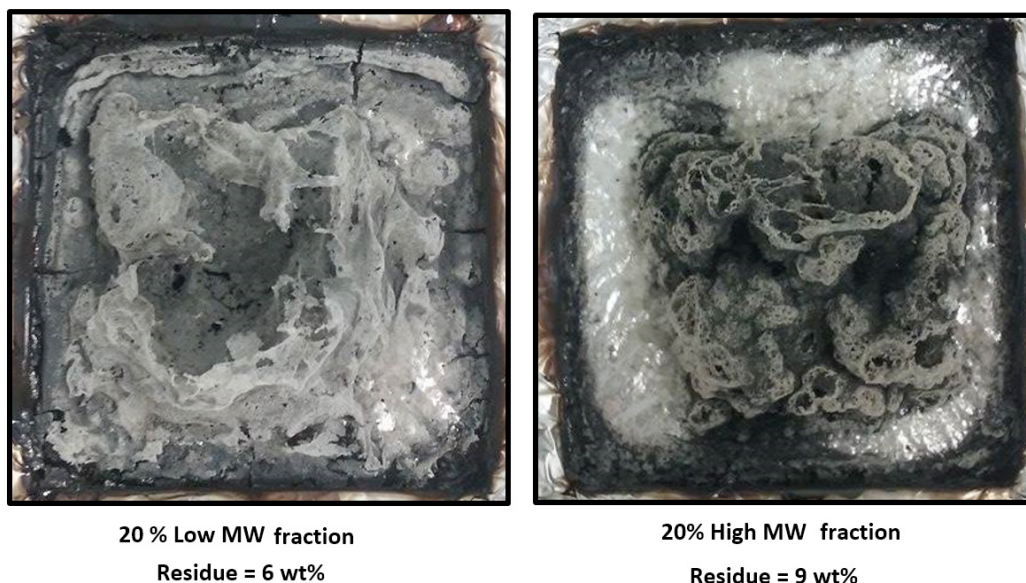Residue = 6 wt%

20% High MW fraction
Residue = 9 wt%

Figure 9: Pictures of the residues of combustion of PLA/20 lignin composites.

4 Conclusion

Two lignin fractions, presenting a specific molecular weight, were obtained from a Kraft lignin by using ultrafiltration membranes method. Their structures and thermal properties were first determined prior to be used as flame retardant additives for PLA. It was highlighted that lignin thermal stability is strongly affected by the presence of oxidized small fragments. These molecules, present in LMW fraction, are responsible for its low thermal stability as well as to its strong combustion.

We have pointed out that the separation of such small lignin fragments presents a real benefit since using HMW fraction enables for obtaining PLA composites presenting enhanced properties, i.e. more thermally stable composite with improved flame retardant behavior.

References

[1] L. Ferry, G. Dorez, A. Taguet, B. Otazaghine, J.M. Lopez-Cuesta, Polym. Degrad. Stab. 113 (2015) 135–143.

[2] A. De Chirico, M. Armanini, P. Chini, G. Cioccolo, F. Provasoli, G. Audisio, Polym. Degrad. Stab. 79 (2003) 139–145.

[3] B. Prieur, M. Meub, M. Wittemann, R. Klein, S. Bellayer, G. Fontaine, S. Bourbigot, Polym. Degrad. Stab. 127 (2016) 32–43.

[4] W. Xing, H. Yuan, P. Zhang, H. Yang, L. Song, Y. Hu, , J. Polym. Res. 20 (2013) 1–12. doi:10.1007/s10965-013-0234-1.

[5] J. Zhang, E. Fleury, Y. Chen, M.A. Brook, Flame retardant lignin-based silicone composites, RSC Adv. 5 (2015) 103907–103914. doi:10.1039/C5RA24093J.

[6] L. Costes, F. Laoutid, M. Aguedo, A. Richel, S. Brohez, C. Delvosalle, Ph Dubois, European Polymer Journal 84 (2016) 652–667

[7] A. A. Alalykin, R. L. Vesnin, and D. A. Kozulin, Russian journal of applied chemistry, 84, 2011, 1616-1622

[8] A. Cayla, F. Rault, S. Giraud, F. Salaün, V. Fierro, A. Celzard, Polymers, 8, 2016, 331

[9] R. Zhang, X. Xiao, Q. Tai, H. Huang, Y. Hu, Polymer engineering and science, 52, 2012, 2620-2626

[10] Y. Yu, S. Fu, P. Song, X. Luo, Y. Jin, F. Lu, Q. Wu, J. Ye, Polymer degradation and stability, 97, 2012, 541-546

[11] L. Costes, F. Laoutid, S. Brohez, Ph. Dubois, Materials Science and Engineering R 117 (2017) 1–25

[12] G. N. G. Lewis, E. Yamamoto, Annual review of plant physiology and plant molecular biology, 41, 1990, 455-496

[13] S.C. Fox, A.G. McDonald, BioResources 5 (2010) 990-1009

[14] S. Laurichesse, L. Avérous, Progress in polymer science, 39, 2014, 1266-1290

[15] A. Vishtal, A. Kraslawski, Bioresources, 6, 2011, 3547-3568

[16] T. Hosoya, H. Kawamoto, S. Saka, J. Anal. Appl. Pyrolysis 84 (2009) 79–83

[17] M. Brebu, T. Tamminen, I. Spiridon, Journal of analytical and applied pyrolysis, 104, 2013, 531-539

[18] M. Brebu, C. Vasile, Cellul. Chem. Technol. 44 (2010) 353–363

[19] J. Zhao, W. Xiuwen, J. Hu, Q. Liu, D. Shen, R. Xiao, Polym. Degrad. Stab. 108 (2014) 133–138

[20] V. Fierro, V. Torné-Fernández, D. Montané, A. Celzard, Thermochim. Acta 433 (2005) 142–148

[21] I. Brodin, E. Sjoholm, G. Gellerstedt, J. Anal. Appl. Pyrolysis 87 (2010) 70–77

[22] J. Hu, D. Shen, S. Wu, H. Zhang, R. Xiao, Journal of analytical and applied pyrolysis, 106, 2014, 118-124

[23] D. J. Nowakowski, J. M. Jones, Journal of analytical and applied pyrolysis, 83, 2008, 12-25

[24] A. Toledano, A. García, I. Mondragon, J. Labidi, Separation and Purification Technology 71 (2010) 38–43

[25] Q. Schmetz, G. Maniet, N. Jacquet, H. Teramura, C. Ogino, A. Kondo, A. Richel, Industrial Crops and Products 94 (2016) 308-317

[26] P. Mousavioun, W.O.S. Doherty, Industrial Crops and Products 31 (2010) 52–58

[27] K. Wang, F. Xu, R. Sun, Int. J. Mol. Sci. 2010, 11, 2988-3001

[28] L. Costes, F. Laoutid, S. Brohez, C. Delvosalle, P. Dubois, European Polymer Journal 94 (2017) 270–285